7C.6 MOMENTUM FLUX STRUCTURES AND STATISTICS IN LOW-WIND MARINE SURFACE LAYERS: OBSERVATIONS AND LARGE-EDDY SIMULATIONS

Peter P. Sullivan[1*], James B. Edson[2], Tihomir Hristov[3], and James C. McWilliams[4]

[1]National Center for Atmospheric Research, Boulder, CO
[2]Department of Marine Sciences, University of Connecticut, Groton, CT
[3]Department of Civil Engineering, Johns Hopkins University, Baltimore, MD
[4]Department of Atmospheric and Oceanic Sciences, UCLA, Los Angeles, CA

1. INTRODUCTION

A primary objective of the Coupled Boundary Layers Air-Sea Transfer low wind (CBLAST Low) program is to investigate the transfer of momentum at low wind speed conditions where the drag coefficients are characterized by significant variability. A large fraction of this uncertainty is believed to be due to sampling variability. However, previous investigations also indicate that physical processes are responsible for some of the scatter seen in direct measurement of the drag coefficients. These studies identify wind-swell interaction and surfactant modulation of the gravity-capillary waves as possible causes. To improve marine forecasts and coupled atmosphere-ocean models, we need to quantify the effects of these physical process and develop parameterizations so as to include their effect in numerical models.

In the present effort, we examine the marine planetary boundary layer (PBL) when the surface layer is in a non-equilibrium state between winds and waves. Specifically we are interested in the impacts of fast moving waves propagating with and against the overlying turbulent flow. Previous observations document unusual characteristics in the wind following wave regime; *e.g.*, low-level jets (Holland et al. 1981; Miller 1999), positive upward momentum flux from the ocean to the atmosphere (Grachev and Fairall 2001; Smedman et al. 1994, 1999; Drennan et al. 1999), and departures from classical wall layer scaling (Rutgersson et al., 2001). These features are signatures of a wave-driven surface layer first reported by Harris (1966). Under ideal conditions with persistent swell leading the winds, LES (Sullivan et al., 2004) predicts that the surface wave motions can induce a low-level jet leading to a turbulence collapse over the bulk of the PBL. Given the potential importance of swell, we interrogate the CBLAST Low observational database searching for wave driven effects with a focus on the vertical momentum transport in the marine surface layer.

corresponding author address: Peter P. Sullivan, National Center for Atmospheric Research, P. O. Box 3000, Boulder, CO 80307-3000; *email*: pps@ncar.ucar.edu

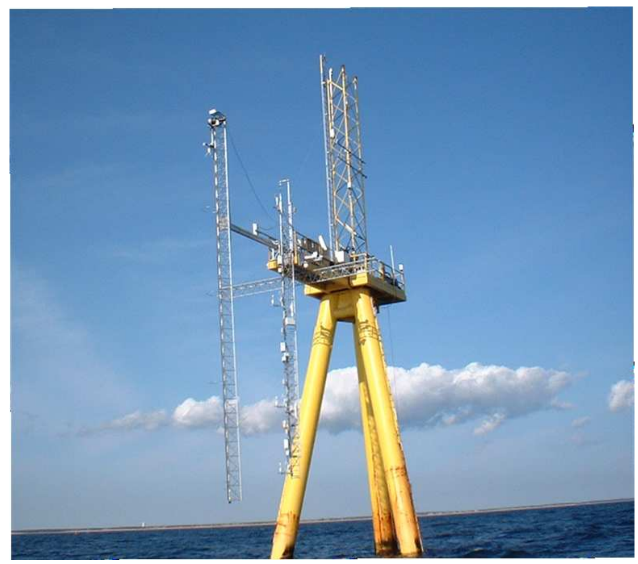

Figure 1: The Air-Sea Interaction Tower with twin masts deployed during the CBLAST low wind field campaign. Sonic anemometers mounted on the forward mast translate vertically to obtain fine spatial resolution of the mean velocity and scalar profiles while fixed sonic anemometers attached to the rearward mast are used to measure vertical (turbulence) fluxes of momentum and scalars.

2. CBLAST LOW OBSERVATIONS

The primary site for the CBLAST low-wind observational program was the coastal region south of Martha's Vineyard openly exposed to the Atlantic Ocean (see CBLAST (2004) for further details). The intensive observation period, approximately two months in duration, occurred in the late summer of 2003 and gathered data using a variety of platforms. One of the novel measuring components is a low-profile air-sea interaction tower (ASIT) which allows detailed turbulence measurements close to the air-water interface (see figure 1). Two vertical masts were deployed from the ASIT: a fixed flux mast designed to gather high resolution turbulence data at four fixed vertical levels and a vertically traversing mast that collected mean profile information over a range of heights above the sea surface. The nominal locations of the flux sonics are $z = [5.85, 7.94, 11.83, 18.1]$m. In addition to the turbulence information a detailed set of wave measurements were also collected (Edson et al., 2004). These datasets allow us to establish links between the turbulent fields and wave state over a range of atmospheric conditions. Here, wave age is defined as the ratio of the phase speed at the peak in the wave height spectrum c_p to the mean wind U_a at a nominal height of $z = 5.85$m above the water. Over the duration of the field campaign the wave age varied from $c_p/U_a = [\sim 1, \sim 10]$.

3. LES OF LOW WIND SURFACE LAYERS

Our computational modeling relies on turbulence resolving direct numerical and large-eddy simulations (DNS and LES) to examine the interactions between winds and waves in the marine surface layer. Sullivan et al. (2000), Sullivan and McWilliams (2002) and Sullivan et al. (2004) describe the simulation technology and interpret the effects of varying wave age and atmospheric stability on marine surface layer dynamics in an idealized setting. In the present work, we continue to analyze our previous LES solutions for turbulent flow above fast moving waves and expand our database to include a wider range of atmospheric stability and wind-wave orientations. During CBLAST Low the surface winds are generally $\sim 5\text{ms}^{-1}$ and the wave fields are frequently dominated by $\sim$100m swell generated by distant fronts. Thus the winds and waves are often in a non-equilibrium state. PBLs dominated by swell are an attractive regime for an LES study as the surface waves are large scale and can be well resolved with reasonable LES meshes. However, simulating the swell regime is computationally demanding as the phase speed of the surface waves is high $c > 10\text{ms}^{-1}$ which places severe limits on the allowable timestep.

Simulations with waves propagating against and at varying angles to the wind are performed using the same input parameters as our previous LES for winds following swell. Specifics of the simulation setup are: computational domain $(1200 \times 1200 \times 800)$m; resolution of the surface fitted grid is $(250 \times 250 \times 96)$ gridpoints with a smoothly varying stretched vertical mesh; geostrophic winds $U_g = 5\text{ms}^{-1}$ and surface roughness $z_o = 2 \times 10^{-4}$m; and, an imposed surface wave with waveslope $ak = 0.1$, phase speed $c = 12.5\text{ms}^{-1}$, and wavelength $\lambda = 100$m. Because of the large value of c, small horizontal grid spacing $\triangle x \sim 4.8$m, and small time-step $\triangle t \sim 0.3$s, the simulations require about 70,000 time-steps (approximately 10 large eddy turnover times) which consumes about 3000 CPU hours per run on an IBM SP4$^+$ using restart volumes archived from previous solutions. In simulations with waves the pressure Poisson equation is solved by an iterative method that adds more than 50% to the computational cost compared to simulations with flat lower boundaries.

4. RESULTS

LES profiles of mean and turbulent variables above swell show significant differences compared with rough wall boundary layers and flow over hills (*i.e.*, stationary waves, see review by Belcher and Hunt (1998)). Our interpretation suggests that this results from momentum flux divergence which accelerates the flow and a retarding pressure gradient both of which are opposite to the momentum balance in classical boundary layers (Sullivan et al., 2004, 2000). The LES is supported by CBLAST observations which provide clear evidence that variability in the drag coefficients at low winds is at least partially explained by this stress-swell interaction mechanism (Sullivan et al., 2004).

Sea state modulates the magnitude and orientation of the mean wind and momentum flux in light winds. Figure 2 compares the horizontal wind field from two LESs with the primary difference being the direction of wave propagation. When winds and waves oppose each other the surface drag increases dramatically slowing the low-level winds and generating vigorous turbulence that fills the entire PBL. Then the mean velocity is positively sheared over the depth of the PBL. The pressure field induced by the waves causes the winds to speedup as they pass over the wave crests and slow down in the wave troughs. For the case with winds following swell the response of the PBL is dramatically different (see lower panel of figure 2). The fastest and slowest surface layer winds now develop over the wave troughs and crests, respectively. Further the waves create a pressure field that induces positive (upward) momentum flux and the formation of a low-level jet at $z \sim [10, 20]$m. The magnitude of the super-geostrophic wind is about $1.1 U_g$; the amplitude and height of the surface jet vary with stratification and surface roughness. Swell propagating in the wind direction then has a significant impact on turbulence in the neutral PBL. In the surface layer, it lowers the mean shear $d\bar{\mathbf{u}}/dz$ and hence weakens the main source of turbulence production for a neutral PBL, $\mathcal{P} = -\overline{\mathbf{u}'w'} \cdot d\bar{\mathbf{u}}/dz$. The absence of a strong turbulence source in the surface layer leads to a turbulence collapse in the overall PBL. This LES prediction in the marine surface layer is supported by the observations of Smedman et al. (1999) who find that turbulence production is significantly reduced in the presence of swell. The state of the near neutral marine PBL, dominated by swell, then becomes sensitive to small amounts of convection.

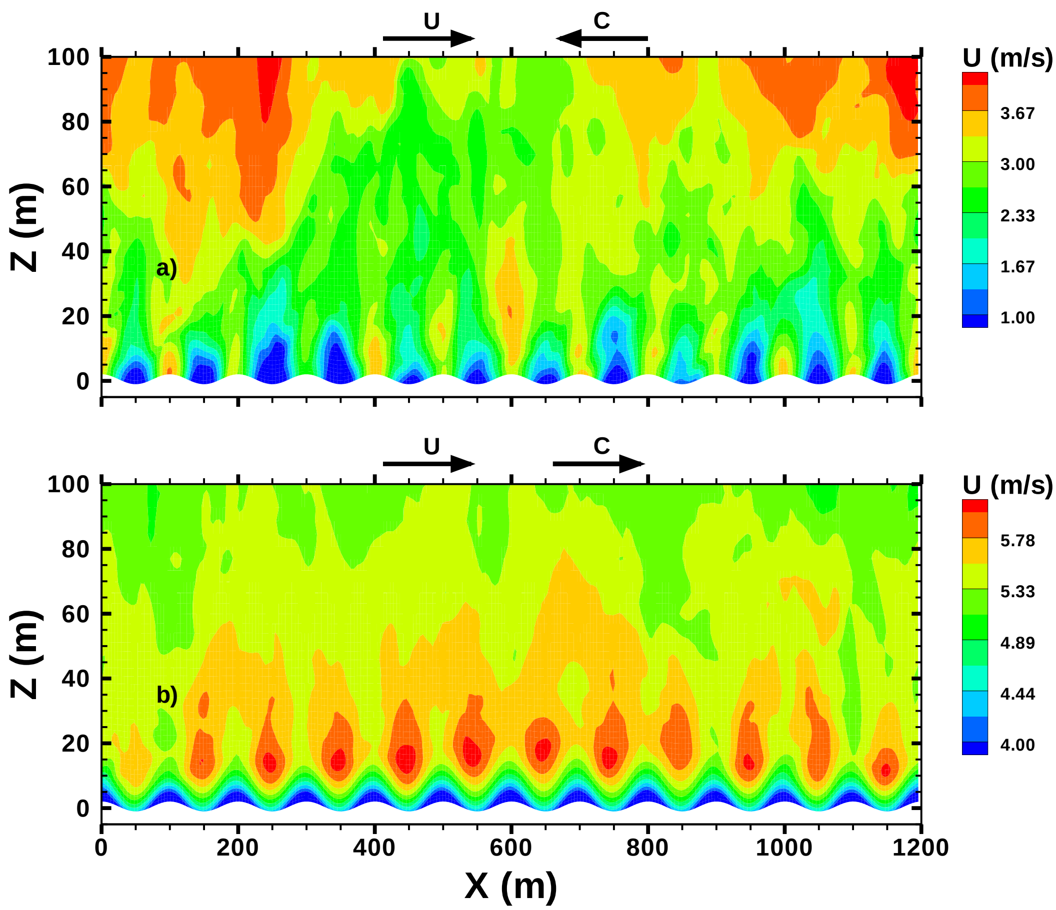

Figure 2: Snapshots of the instantaneous horizontal wind field in $x-z$ planes illustrating the effect of wave propagation direction on the winds in the lowest 100m of the marine boundary layer. In a) waves are propagating right-to-left against the wind while in b) waves are propagating left-to-right with the wind. In a) the surface winds speed up over the wave crests and slow down in the wave troughs while in b) a weak near surface jet forms slightly above the wave troughs and the winds slow over the wave crests. For each simulation the geostrophic wind $U_g = 5\text{ms}^{-1}$, wave phase speed $c = 12.5\text{ms}^{-1}$, wavelength $\lambda = 100$m, and the waveslope $ak = 0.1$. Note the range of the color bar changes between a) and b).

LES also predicts that well organized surface waves impact both the instantaneous and net vertical momentum flux in the PBL. Waves leave their imprint on the coherent flux carrying structures as illustrated in figure 3. Here we compare cases with the same large scale forcing and surface roughness but varying wave fields; no waves, waves propagating with the wind, and waves propagating against the wind. Inspection of the flow visualization at a height of $z = 20$m shows a dramatic response of the PBL. Over a flat lower boundary the bulk of the vertical momentum flux is carried by a few sparsely distributed structures elongated in the mean wind direction (*e.g.*, Lin et al., 1996; Hommema and Adrian, 2003). Fast moving swell propagating with or against the wind destroys the coherence of these streaky near wall structures. For winds following waves, the momentum flux structures in the surface layer are weak and carry slightly positive flux. This is in sharp contrast to the situation of waves propagating against the wind which generates vigorous momentum flux of both signs (see panel c) of figure 3). $u'w'$ induced by the waves remains coherent well above the surface layer and appears to interact with the background PBL turbulence. In this situation the net momentum flux is negative and its fluctuating value noticeably exceeds its mean value.

Our LES show that the turbulence fluxes and variances as well as the mean profiles depend on bulk properties of the wave field, *i.e.*, the wave age, wind-wave orientation, and amplitude of the wave components. The computational results provide motivation to search for wave

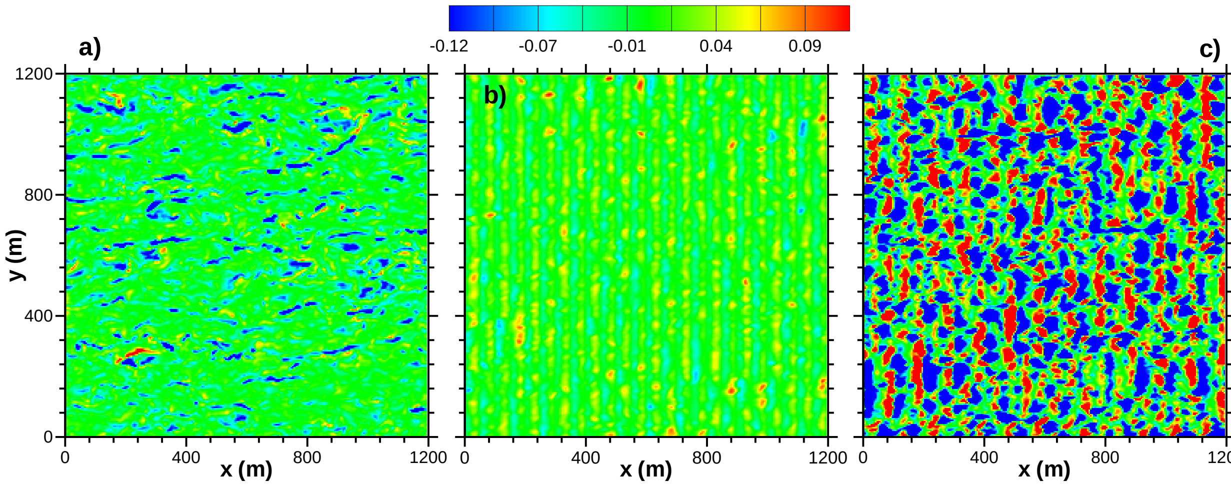

Figure 3: $x - y$ slices showing the instantaneous vertical momentum flux $u'w'$ at a height $z = 20$m above the water. Panel a) is turbulent flow over parameterized roughness $z_o = 0.0002$m and no surface waves. Panel b) is flow over swell traveling with the wind and c) is flow over swell traveling against the wind. The wave conditions are as shown in figure 2. The color bar for momentum flux is in units of $(\mathrm{ms}^{-1})^2$.

influences in measured wind fields from the CBLAST field campaign. Compared to a fully developed sea, the wave fields in the LES are highly idealized, *e.g.,* they do not include multi-components, three-dimensionality, and time varying wave amplitudes and phases. Hence, we expect wave influences to be more subtle and difficult to isolate in observations. A statistical measure we find useful to help identify wave effects is a quadrant analysis of the vertical momentum flux. This technique, first used by Antonia and Chambers (1980) and later by Smedman et al. (1999) separates the turbulent momentum flux $u'w'$ into four categories (quadrants) according to the sign of the two fluctuating velocity components (see figure 4).

In the surface layer of a rough wall boundary layer the net (average) momentum flux $\langle u'w' \rangle < 0$ and is dominated by sweeps and ejections associated with motions in quadrants Q2 and Q4. Positive flux contributions from quadrants Q1 and Q3 are less frequent and weaker in magnitude. We performed a quadrant analysis of the vertical momentum flux in the marine surface layer using CBLAST data with the expectation that the influence of swell would appear at sufficiently high wave age. The results of the analysis are displayed in figure 5 where we show the (normalized) ratio of negative to positive momentum flux quadrants $Q_r = -(Q2+Q4)/(Q1+Q3)$ for varying wave age c_p/U_a.; observational results for flow over stationary roughness (Sullivan et al., 2003) are also depicted for comparison. A wide range of atmospheric stratification is considered but the results are restricted to situations where the winds and waves are aligned within ± 30 degrees. The results contain scatter but the quadrant flux ratio shows wave influences, a distinct downward trend for increasing wave age $c_p/U_a > 1$. Our interpretation, based on our LES results, is that the fast moving components of the wave field enhance the upward momentum transport from the ocean to the atmosphere and this momentum appears in the positively signed flux quadrants $(Q1, Q3)$. At a sufficiently large wave age a near balance between negative and positive flux contributions is achieved. This result is quite similar to the predictions from direct numerical simulations (Sullivan et al., 2000) and from LES (see figure 3). Notice also that the effects of fast moving waves on momentum transport are not confined to the first measurement level $z = 5.85$m but appear to extend over the bulk of the surface layer, up to at least $z = 18.1$m. The observations from Smedman et al. (1999) also follow a similar trend with wave age.

The CBLAST Low data supports the LES predictions and both are suggestive that swell under a certain range of conditions can modify the turbulence structures responsible for momentum transport in the marine surface layer. The impact of swell is expected to increase with the amplitude and coherence of the waves. For the bulk of the CBLAST Low observations the significant wave height is low $H_s < 1.5$m. The swell signature is more pronounced in the presence of larger waves as shown by Miller (1999).

5. DISCUSSION AND CONCLUSIONS

There is a striking resemblance between the present LES solutions and observations of swell dominated marine boundary layers. The formation of a jet or in some instances a near uniform velocity profile in the vicinity

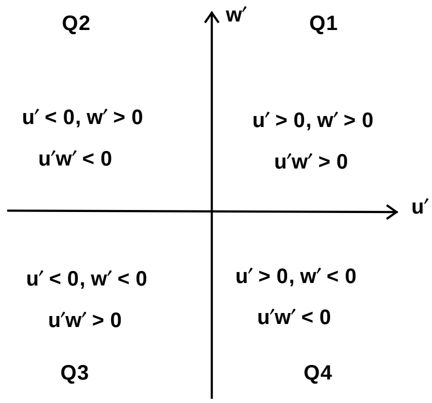

Figure 4: Decomposition of the vertical momentum flux into quadrants (Q1, Q2, Q3, Q4) based on the sign of the fluctuating horizontal and vertical velocity (u', w').

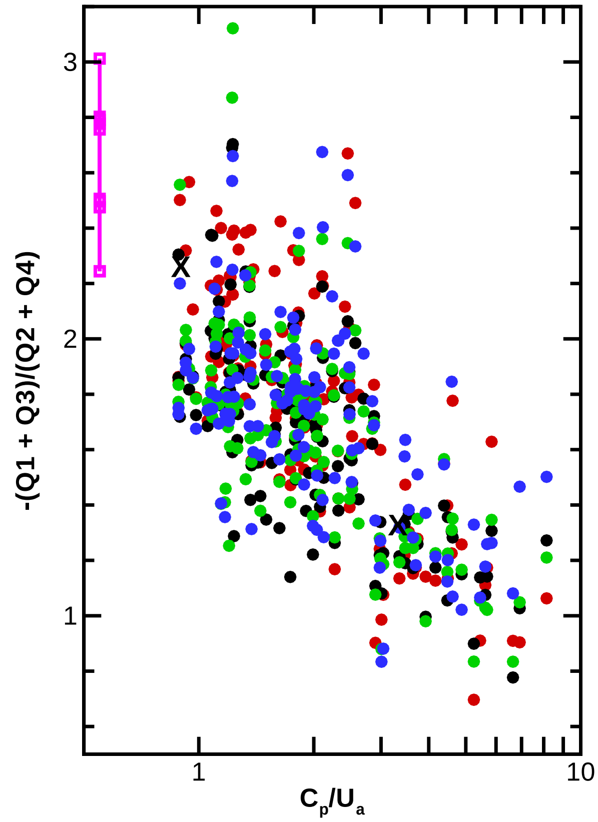

Figure 5: Quadrant analysis of the vertical momentum flux in the marine surface layer for varying wave age from CBLAST Low. Solid circles are measurements at z =(5.85 •, 7.94 •, 11.8 •, 18.1 •)m. The observations of Smedman et al. (1999) are denoted by **X** and results for flow over stationary roughness (note wave age = 0) (Sullivan et al., 2003) are indicated by open squares.

of the waves is consistent with past and current surface layer observations of Holland et al. (1981), Miller (1999) and Edson et al. (2004). These investigations find that the region influenced by swell can exceed the height of the measuring mast, approximately $0 < z < 15$m. Hence, LES and observations both find that swell leading the wind invalidates the notion of a shallow wave boundary layer. The influence of swell is not confined to the surface layer. Fast moving swell upsets the turbulence production mechanism in the marine surface layer which in turn impacts the whole PBL. In the absence of shear production, turbulence in the upper PBL tends to collapse and the wave-driven PBL differs from its counterpart with stationary surface roughness. Thus the LES supports some of the findings reported by Smedman et al. (1994, 1999). The appearance of a low-level jet and vertically varying vertical momentum flux make surface layer measurements dependent on wave state and vertical distance above the surface thus invalidating the Monin-Obukhov method of predicting surface fluxes in agreement with Rutgersson et al. (2001).

LES predicts sea state modulates the important structures that transmit vertical momentum flux between the atmosphere and ocean. For winds following and opposing the wave field the primary flux carriers are associated with the waves. When the waves oppose the wind the instantaneous vertical momentum flux greatly exceeds its mean value. A quadrant analysis of the vertical momentum flux from the CBLAST Low database shows a wave signature. With strong swell the distribution of positive momentum flux in quadrants $(Q1, Q3)$ approaches that contained in the negative momentum quadrants $(Q2, Q4)$. Thus marine surface layers with non-equilibrium winds and waves contain unique features compared to their terrestrial counterparts.

The present results can be used to help interpret the observations of bulk air-sea fluxes. The measurements of the neutral drag coefficient C_D obtained during CBLAST Low (see figure 6) agree well with the TOGA-COARE algorithm (Fairall et al., 2003; Edson et al., 2006) over a wide range of wind speeds. The greatest discrepancy (and variability) occurs at low winds where the measured values of C_D can be either positive or negative with amplitudes exceeding the average estimate by a factor of two or more. At low winds, say $U_a < 5\mathrm{ms}^{-1}$, LES predicts swell induces a significant change in the vertical momentum flux. Swell propagating with the winds reduces the observed momentum flux (or even changes its sign) while the same swell propagating counter to the winds greatly enhances the surface drag. The model predictions suggest that the impact of non-equilibrium seas

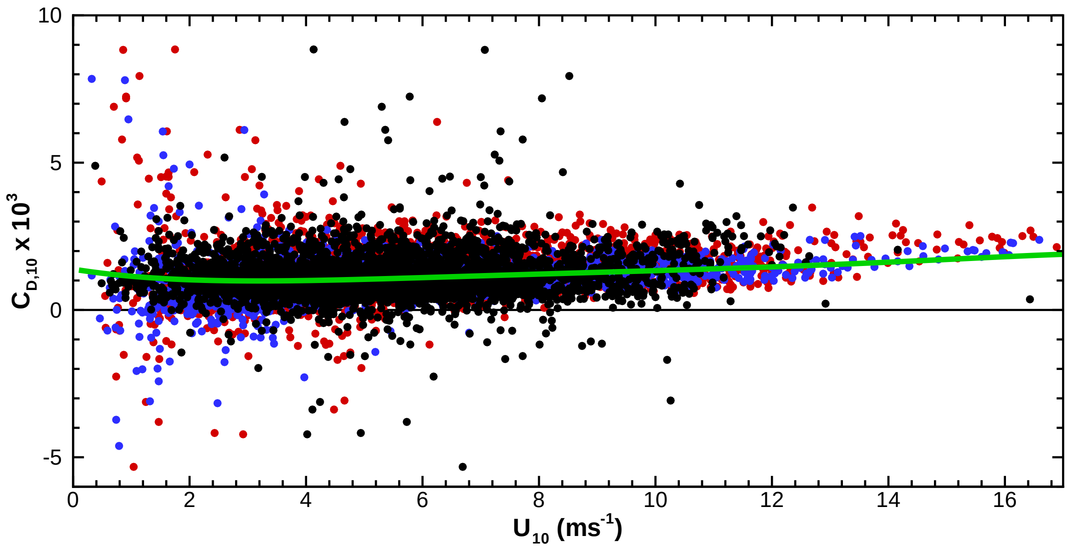

Figure 6: Drag coefficients obtained from three measurement levels during CBLAST Low (Edson et al., 2006). C_D is referenced to a 10m height and neutral conditions. The TOGA COARE 3.0 parameterization is indicated by the solid green line. Note the negative values of C_D and increase in variability at low winds.

can cause large variability in measured drag coefficients at low winds. This effect is not considered in the TOGA COARE algorithm (Fairall et al., 2003).

The current LES with its monochromatic wave represents an idealization of a light wind PBL with swell. In the open ocean, a multi-component wave field can simultaneously be a sink and source of momentum for the atmosphere, with short (long) waves extracting (imparting) momentum. The sign and magnitude of the near surface fluxes will then depend on several factors including the orientation of winds and waves and the relative location of the wave spectral peak and the mean wind. Flux parameterizations thus require information about the wave field in addition to the winds.

Acknowledgments: NCAR is sponsored by the National Science Foundation. This work is supported by the CBLAST Initiative of the Office of Naval Research.

REFERENCES

Antonia, R. A. and A. J. Chambers, 1980: Wind-wave-induced disturbances in the marine surface layer, *J. Phys. Oceanogr.*, **10**, 611–622.

Belcher, S. E. and J. C. R. Hunt, 1998: Turbulent flow over hills and waves, *Annual Review of Fluid Mechanics*, **30**, 507–538.

CBLAST, 2004: http://www.whoi.edu/science/aope/dept/cblast/low/cblastlow.html.

Drennan, W. M., K. K. Kahma, and M. A. Donelan, 1999: On momentum flux and velocity spectra over waves, *Boundary-Layer Meteorol.*, **92**, 489–515.

Edson, J. B., R. F. Crofoot, W. R. McGillis, and C. Zappa, 2004: Investigations of flux-profile relationships in the marine atmospheric surface layer during CBLAST, in *16th Amer. Meteorol. Soc. Symp. on Boundary Layers and Turb.*, Portland, ME.

Edson, J. B., C. W. Fairall, and P. P. Sullivan, 2006: Evaluation and continued improvements to the TOGA COARE 3.0 algorithm using CBLAST data, in *27th Amer. Meteorol. Soc. Symp. on Hurricanes and Tropical Meteorology*, Monterey, CA.

Fairall, C. W., E. F. Bradley, J. E. Hare, A. A. Grachev, and J. B. Edson, 2003: Bulk parameterization of air-sea fluxes: Updates and verification for the COARE algorithm, *J. Clim.*, **16**, 571–591.

Grachev, A. A. and C. W. Fairall, 2001: Upward momentum transfer in the marine boundary layer, *J. Phys. Oceanogr.*, **31**, 1698–1711.

Harris, D. L., 1966: The wave-driven wind, *J. Atmos. Sci.*, **23**, 688–693.

Holland, J. Z., W. Chen, J. A. Almazan, and F. C. Elder, 1981: Atmospheric boundary layer, in *IFYGL-The international field year for the Great Lakes*, edited by E. J. Aubert and T. L. Richards, pp. 109–167, NOAA, Ann Arbor, MI.

Hommema, S. E. and R. J. Adrian, 2003: Packet structure of surface eddies in the atmospheric boundary layer, *Boundary-Layer Meteorol.*, **106**, 147–170.

Lin, C.-L., J. C. McWilliams, C.-H. Moeng, and P. P. Sullivan, 1996: Coherent structures and dynamics in a neutrally stratified planetary boundary layer flow, *Phys. Fluids*, **8**, 2626–2639.

Miller, S. D., 1999: *The structure of turbulent and wave-induced wind fields over open-ocean waves*, Ph.D. thesis, University of California Irvine.

Rutgersson, A., A. Smedman, and U. Högström, 2001: Use of conventional stability parameters during swell, *J. Geophys. Res.*, **106**, 27117–27134.

Smedman, A., U. Högström, H. Bergström, and A. Rutgersson, 1999: A case study of air-sea interaction during swell conditions, *J. Geophys. Res.*, **104**, 25833–25851.

Smedman, A., M. Tjernström, and U. Högström, 1994: The near-neutral marine atmospheric boundary layer with no surface shearing stress: A case study, *J. Atmos. Sci.*, **51**, 3399–3411.

Sullivan, P. P., J. B. Edson, J. C. McWilliams, and C.-H. Moeng, 2004: Large-eddy simulations and observations of wave driven boundary layers, in *16th Amer. Meteorol. Soc. Symp. on Boundary Layers and Turbulence*, Portland, ME.

Sullivan, P. P., T. W. Horst, D. H. Lenschow, C.-H. Moeng, and J. C. Weil, 2003: Structure of subfilter-scale fluxes in the atmospheric surface layer with application to large-eddy simulation modeling, *J. Fluid Mech.*, **482**, 101–139.

Sullivan, P. P. and J. C. McWilliams, 2002: Turbulent flow over water waves in the presence of stratification, *Phys. Fluids*, **14**, 1182–1195.

Sullivan, P. P., J. C. McWilliams, and C.-H. Moeng, 2000: Simulation of turbulent flow over idealized water waves, *J. Fluid Mech.*, **404**, 47–85.